ISSN : 0974 - 7486 Volume 8 Issue 3

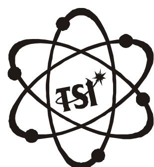

Materials Science

Trade Science Inc.

An Indian Journal

Full Paper

MSAIJ, 8(3), 2012 [107-112]

Effect of substrate temperature on whisker growth of electron-beam-evaporated indium tin oxide

S.N.Alamri

Department of Physics, Science Faculty, Taibah University, Madinah, P.O.Box:30002, (SAUDI ARABIA)

E-mail: alamrisaleh@yahoo.com

Received: 12th July, 2011 ; Accepted: 12th August, 2011

ABSTRACT

Thin films of indium tin oxide (ITO) were deposited on soda-lime glass with the electron beam technique at substrate temperatures between 50°C and 300°C. Properties that were characterised include structure, surface morphology, resistivity, mobility, transmittance, reflectance, and optical band gap. Structural characterization was performed using scanning electron microscopy and X-ray diffraction. Elevating the substrate temperatures from 50°C to 300°C, increased the thickness of ITO films more than three times by increasing the grain size. The microstructure of the ITO film changed from amorphous to polycrystalline as a function of increasing substrate temperature. The transmittance of the film increased, despite the increasing thickness, and the reflectance was reduced. The optical band gap, E_g, increased from 3.8 eV for the film deposited at 150°C to 3.94 eV for the film deposited at 300°C. The resistivities and mobilities of the fabricated films decreased and increased, respectively, up to 250°C and then deteriorated at 300°C, which could be due to the formation of the observed whiskers.

© 2012 Trade Science Inc. - INDIA

KEYWORDS

Indium tin oxide;
Electron beam technique;
Whiskers;
Substrate temperature.

INTRODUCTION

Sn-doped indium (ITO), a transparent conductor, is an important material in the field of optoelectronic devices such as solar cells[1], liquid crystal displays, plasma displays[2], light-emitting diodes[3], and smart windows[4]. A variety of deposition techniques have be used to fabricate ITO layers, such as reactive thermal evaporation[5], electron beam evaporation[6], DC and RF sputtering[7, 8], pulsed laser ablation[9], sol-gel processing[10], dip coating, and spray pyrolysis[11]. The majority of studies investigating ITO deposition have been concerned with films prepared by sputtering, and there is little published data on other methods[12]. The electron beam evaporation technique is a promising method for producing ITO films with lower resistivities and higher transmittances[13]. The electrical and optical properties of ITO films obtained using electron beam evaporation strongly depend on preparation methods and conditions[14].

This study investigates the effects of substrate temperature on the properties of ITO films produced

by electron beam deposition.

EXPERIMENTAL PROCEDURE

ITO thin films were deposited onto standard soda-lime microscope-slide glass using an Edwards Auto306 electron beam-coating unit. The target material (In_2O_3-SnO_2, 90-10 wt%, typically 99.99% pure, 3-12 mm pieces) was obtained from CERAC™, Incorporated. The investigated substrate temperatures included 50°C, 100°C, 150°C, 200°C, 250°C, and 300°C. The system was pumped down to a base pressure of less than 10^{-6} mbar. The time of deposition was 45 min and the current of the filament increased from 5 mA to 25 mA at an acceleration voltage of 5 kV. Figure 1 depicts the time periods of the increasing filament current. The thickness and the morphologies of the ITO films were observed by scanning electron microscopy (SEM) (Shimadzu SuperScan SSX-550 scanning electron microscope).

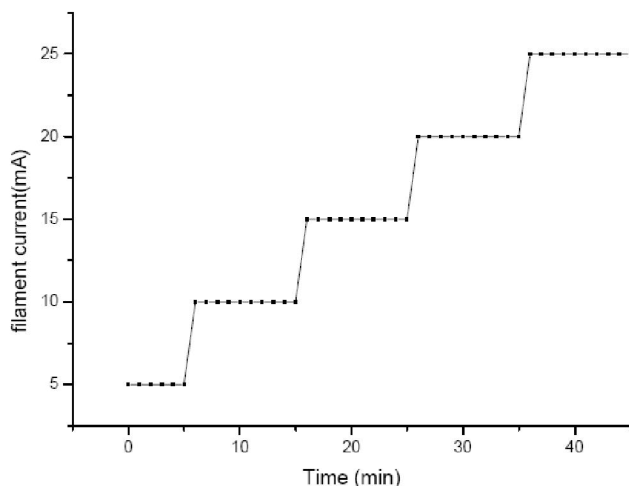

Figure 1 : Time periods of the increasing filament current.

The transmittance, $T(\lambda)$, and reflectance, $R(\lambda)$, spectra of the deposited films were measured at the normal and at a 5° incident angle to the surfaces of the films, respectively. These measurements were acquired in air at room temperature in the spectral range of 190 to 2500 nm using a double-beam spectrophotometer (Shimadzu 3150 UV-VIS-NIR) with a resolution of 0.1 nm. The structure of the ITO film was examined using a Shimadzu XRD-6000 X-ray diffractometer using *Cuk*α radiation (λ=1.5418Å) with an Anton Paar HTK1200N high-temperature oven-chamber attachment. The X-ray tube voltage and current were maintained at 40 kV and 30 mA, respectively. The X-ray diffraction measurements were taken at room temperature for the samples deposited at different substrate temperatures and at different temperatures for the sample deposited at 50°C. The Hall effect and electrical resistivity were measured using a van der Pauw configuration using an ECOPIA Hall effect measurement system (HMS-3000).

RESULTS AND DISCUSSION

Deposition rate and structure

Figure 2 depicts the dependence of ITO film thickness on substrate temperature. The ITO film thickness was observed to increase from 360 nm to 1270 nm as the substrate temperature was increased from 50°C to 300°C. The observed increases in film thickness was due to increasing grain size as a function of temperature, as shown in the cross-sectional microstructure of the fabricated film depicted in Figure 3. The films deposited at 50°C appear denser, and the grain structure is not obvious, suggesting that the film is fully amorphous[15]. The film deposited at 300°C consists of fibre-shaped whiskers, which are easier to see from the cross-sectional view of the film at the surface. The surface morphologies of ITO films deposited at different substrate temperatures are shown in Figure 4. The surface of the film deposited at 50°C was a smooth, solid, and contained several ball-like objects. These balls increased in number and covered the entire surface of

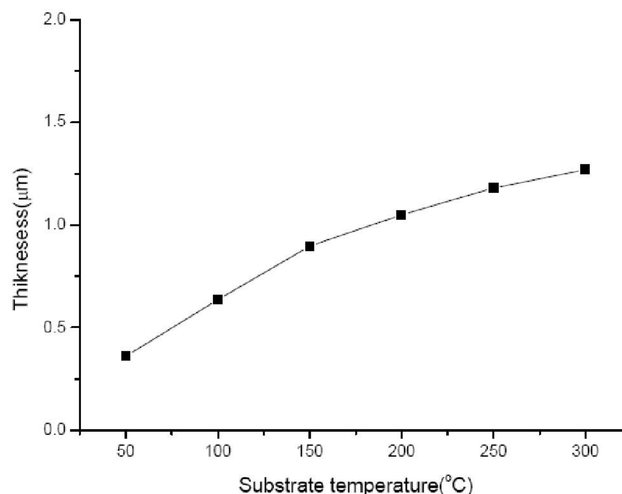

Figure 2 : Dependence of ITO film thickness on substrate temperature.

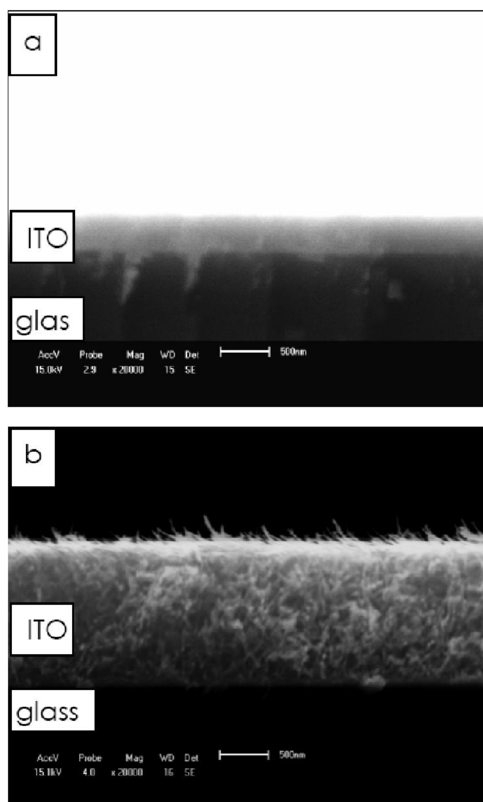

Figure 3 : Cross-sectional images of films deposited at (a) 50°C and (b) 300°C.

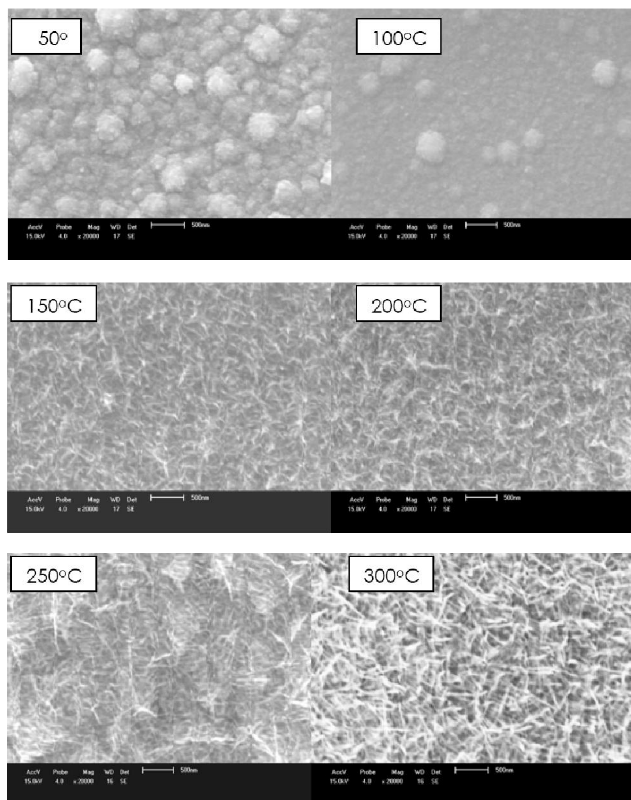

Figure 4 : SEM images of ITO films deposited at different substrate temperatures.

the films deposited at 100°C, and were observed to grow together at higher temperatures. At the highest temperature, 300°C, the film became completely covered by whisker-like projections[16].

The fundamental mechanism of whisker growth is still not fully understood, although several mechanisms have been proposed. One of these mechanisms is called the VLS mechanism[17]. According to this mechanism, a Sn-rich droplet is supersaturated by vapour molecules such that In_2O_3 precipitates and VLS whiskers of In_2O_3 are able to grow[16]. Many theories agree that compressive stresses[18, 19] provide the driving force for whisker formation. The source of compressive stress originates from mechanical, thermal, and chemical processes[20, 21]. Then the substrate temperature can increase the compressive stress, as thermal process, which provides the driving force for whisker formation.

Figure 5 depicts the X-ray diffraction spectra of the ITO samples deposited at different substrate temperatures. No peak was observed in the sample deposited at 50°C, indicating that the film was entirely amorphous. As substrate temperature was increased, diffraction peaks appeared at (400), (222), (211), and (622)[16, 22] and became more intense. These spectra indicate that the crystallinity of the films improved and individual crystallite size increased as a function of elevated substrate temperatures[23]. In order to compare the effect of substrate deposition temperature to post-deposition annealing on the structures of the films, X-ray diffraction spectra were measured for the sample deposited at 50°C and annealed in the oven chamber

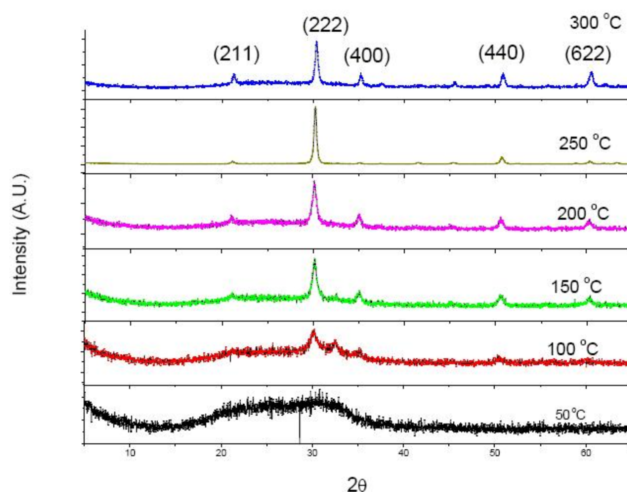

Figure 5 : X-ray diffraction patterns of the ITO films deposited at different substrate temperatures.

Full Paper

at different annealing temperatures: 50°C, 100°C, 150°C, 200°C, 250°C, and 300°C. According to Figure 6, it is clear that annealing induced a transition in the film from amorphous to polycrystalline similarly as was observed by depositing at higher substrate temperatures; however, this transition was first observed at 150°C for the annealing process in comparison to a substrate deposition temperature of 100°C.

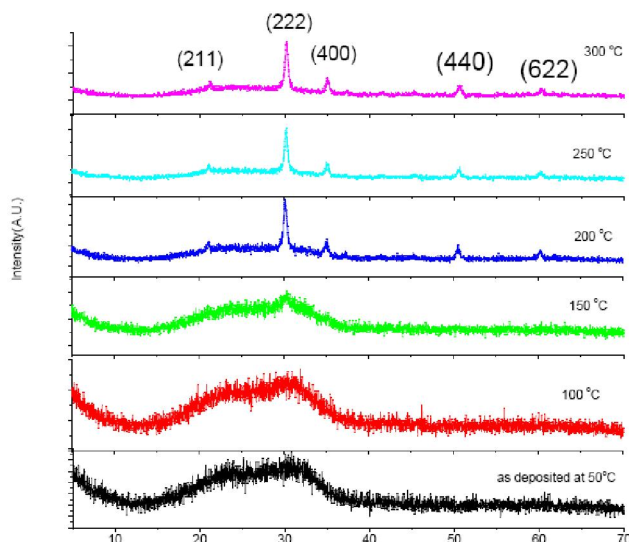

Figure 6 : X-ray diffraction patterns of ITO films annealed at different temperatures.

The grain size, D, of the crystallites was calculated using Sherrer's formula[24]:

$$D = \frac{S\lambda}{\beta \cos\theta} \quad (1)$$

where S is the Scherrer constant and is equal to 0.9, λ is the wavelength of the X-ray and is equal to 1.54 Å for Cukα radiation, θ is the diffracted angle, and β is the full width at half-maximum of the respective peak in radians.

Substrate deposition temperature was observed to increase grain size more than annealing, as shown in Figure 7; hence, temperature affected the grain size of the thin film more during deposition than during post-deposition annealing. In general, grain size increased rapidly in both cases up to 200°C and then increased at a lower rate for higher temperatures.

Optical and electrical properties

Figure 8 and 9 demonstrate that increasing substrate temperatures increased the transmittance and reduced the reflectance of the fabricated films. The transmittance of the film increased despite an increasing film thickness

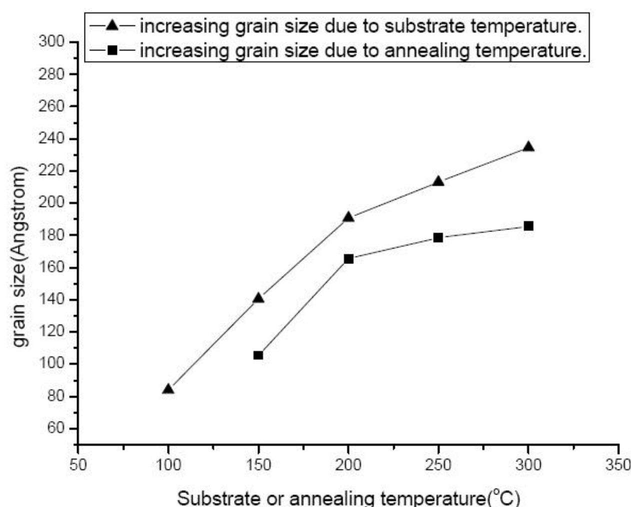

Figure 7 : Grain size as a function of substrate deposition temperature and annealing temperature.

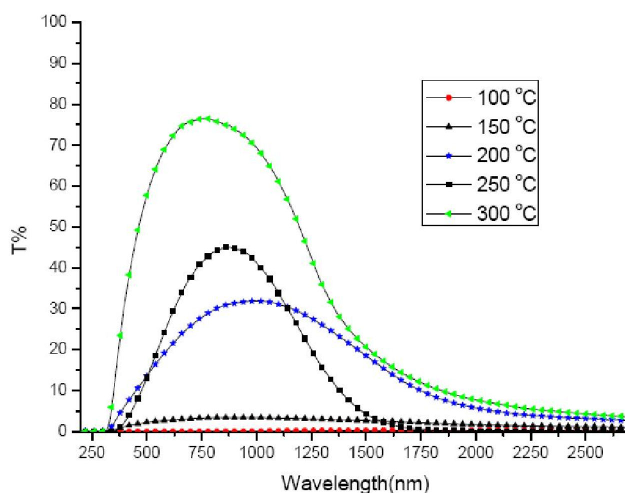

Figure 8 : Transmittance of the films deposited at different substrate temperatures.

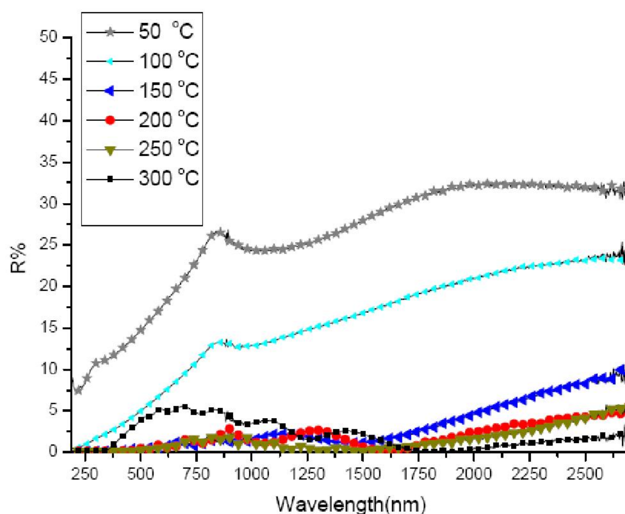

Figure 9 : Reflectance of the films deposited at different substrate temperatures.

as a function of temperature. The films that were deposited at low substrate temperatures of 50°C, 100°C, and 150°C were nearly opaque. In contrast, the transmittance of the film deposited at 300°C was 76% at a wavelength of 751 nm.

The optical band gaps, E_g, of the transparent films were evaluated to investigate the effect of substrate temperature on the optical band gap using the following equation[25]:

$$\alpha(h\upsilon) = A(h\upsilon - E_g)^{1/2} \quad (2)$$

Absorption coefficients, $\alpha(h\upsilon)$, were calculated for the transparent films using the following formula[26]:

$$\alpha(\lambda) = \frac{1}{d}\ln\left[\frac{(1-R(\lambda))^2}{T(\lambda)}\right] \quad (3)$$

where d is the film thickness, R is the reflectance, and T is the transmittance.

Using Eq. 3, the direct-allowed transitions, α^2, vs. photon energy, $h\upsilon$, were plotted (Figure 10) for the transparent films deposited with substrate temperatures of 150°C, 200°C, 250°C, and 300°C. The intercept on the x-axis gives the value of the optical band gap, E_g, which increased from 3.8 eV for the film deposited at 150°C to 3.94 eV for the film deposited at 300°C.

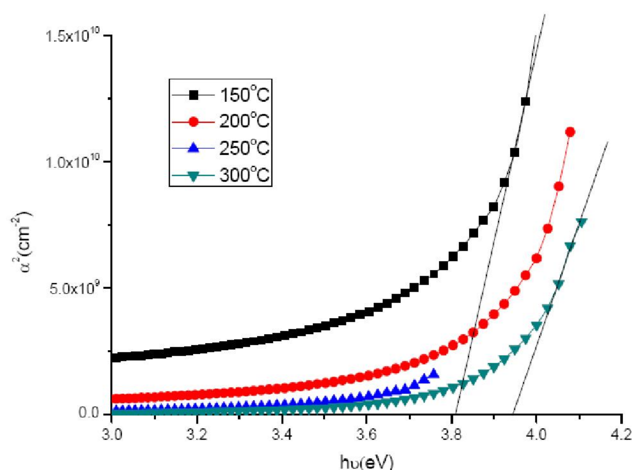

Figure 10 : The square of the absorption coefficient (α2) as a function of the photon energy (eV) for ITO films deposited at 150°C, 200°C, 250°C, and 300°C.

The dependence of film resistivity and carrier mobility on deposition substrate temperature is indicated in Figure 11. Therein, the resistivity can be observed to decrease with increasing substrate temperature from 50°C up to 250°C, and then increased at 300°C. The opposite phenomenon was observed for carrier mobility, that is, film resistivity decreased while mobility increased up to 250°C due to the carrier transport enhancement caused by the crystallization of the films[13]. The increase in film resistivity and decrease in mobility at 300°C could be due to the morphology of the film. As shown in Figures 3 and 4, the film deposited at 300°C consisted of fibre-shaped whiskers. Migration of the atoms through the bulk and the surface of the film to create the whiskers could have caused defects in the film, which in turn, would deteriorate the physical properties of the film (e.g., resistivity and mobility).

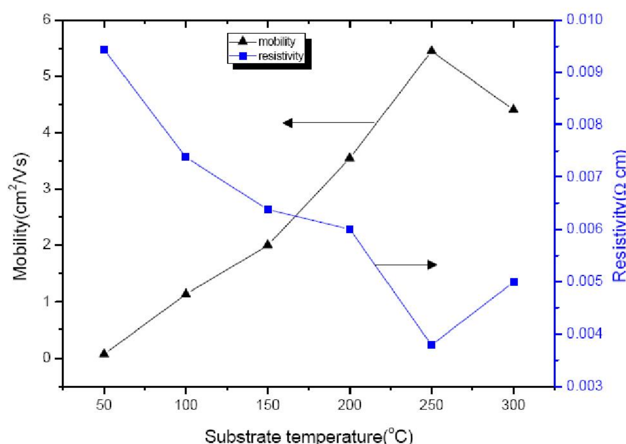

Figure 11 : Resistivity and mobility of the ITO thin films as a function of substrate temperature.

CONCLUSIONS

The experimental results in this work indicate that substrate temperature strongly influences the resistivity and mobility of ITO films deposited by the electron beam technique. The substrate temperature changes the microstructure of the film, which in turn, changes most of the physical properties. The film deposited at 50°C was fully amorphous and was observed to begin transitioning to a polycrystalline phase at a substrate deposition temperature of 100°C, wherein the grain size was observed to increase from 83.9 to 234.7 Å for the film deposited at 300°C.

The film deposited at 300°C consisted of fibre-shaped whiskers, indicating that the elevated substrate temperature could be the source of the compressive stress that provides the driving force for whisker formation. The growth of whiskers affects the distribution of atoms throughout the film, causing defects in the film, which in turn, increase film resistivity and decrease

Full Paper

mobility. This phenomenon could explain why resistivity increases and mobility decreases in films deposited with substrate temperatures of 300°C.

Increasing the substrate temperature improved the optical properties of ITO films by increasing their transmittance and reducing their reflectance. The optical band gap, E_g, increased from 3.8 eV for the film deposited at 150°C to 3.94 eV for the film deposited at 300°C.

ACKNOWLEDGEMENTS

We wish to thank the Deanship of Scientific Research at Taibah University who financially supported this work under contracted research project 429/227.

REFERENCES

[1] Jae-Hyeong Lee, Dong-Gun Lim, Jun-Sin Yi; Solar Energy Materials & Solar Cells, **75**, 235-242 **(2003)**.

[2] I.Hamburg, C.G.Granvist; J.Appl.Phys., **60**, R123 **(1986)**.

[3] I.D.Parker; J.Appl.Phys., **75**, 1656 **(1994)**.

[4] G.C.De Vries; Electrochimica.Acta., **44**, 3185-3193 **(1999)**.

[5] H.U.Habermeier; Thin Solid Films, **70**, 157 **(1981)**.

[6] P.Manivannan, Subrahmanyam; J.Phys.D.Appl. Phys., **26**, 1510-1515 **(1993)**.

[7] K.Utsumi, H.Ligusa, R.Tokumaru, P.K.Song, Y.Shigesato; Thin Solid Films, **445**, 229-234 **(2003)**.

[8] K.Zhang, F.Zhu, C.Huan, A.Wee; Thin Solid Films, **376**, 255-263 **(2000)**.

[9] F.O.Adurodiji, H.Izumi, T.Ishihara, K.Yamada, H.Matsui, M.Motoyama; Thin Solid Films, **350**, 79 **(1999)**.

[10] M.J.Alam, D.C.Cameron; Thin Solid Films, **420-421**, 76-82 **(2002)**.

[11] H.El Rhaleb, E.Benamar, M.Rami, J.P.Roger, A.Hakam, A.Ennaoui; Applied Surface Science, **201**, 138-145 **(2002)**.

[12] M.Mizuhashi; Thin Solid Films, **76**, 97-105 **(1981)**.

[13] J.George, C.S.Menon; Surf.Coat.Technol., **132**, 45 **(2000)**.

[14] M.Yamaguchi, A.Ide-Ektessabi, H.Nomura, N.Yasui; Thin Solid Films, **447-448**, 115-118 **(2004)**.

[15] D.C.Paine, T.Whitson, D.Janiac, R.Beresford, C.O.Yang; J.Appl.Phys., **85(12)**, 8445 **(1999)**.

[16] H.Yumoto, J.Hatano, T.Watanabe, K.Fujikawa, H.Sato; Jpn.J.Appl.Phys., **32**, 1204 **(1993)**.

[17] R.S.Wagner, W.C.Ellis; Trans.Met.Soc.AIME, **233**, 1053 **(1965)**.

[18] K.W.Moon, C.E.Johnson, M.E.Williams, O.Kongstein, G.R.Stafford, C.A.Handwerker, W.J.Boettinger; Journal of Electronic Materials, **34(9)**, L31 **(2005)**.

[19] T.H.Chuang, C.C.Chi, H.J.Lin; Metallurgical and Materials, **39A**, 604 **(2008)**.

[20] Y.W.Lin, Y.Lai, Y.L.Lin, C.Tu, C.R.Kao; Journal of Electronic Materials, **37(1)**, 17 **(2008)**.

[21] M.Chen, S.Ding, Q.Sun, D.W.Zhang, L.Wang; Journal of Electronic Materials, **37(6)**, 894 **(2008)**.

[22] A.Kachouance, M.Addou, A.Bougrine, B.EI idrissi, R.Messoussi, M.Regragui, J.Bernede; Material Chemistry and Physics, **70**, 285 **(2001)**.

[23] J.Ma, D.Zhang, S.Li, J.Zhao, H.Ma; Jpn.J.Appl. Phys., **37**, 5614 **(1998)**.

[24] L.I.Maissel, R.Glang; Hand Book of Thin Film Technology, McGraw-Hill, New York, **(1980)**.

[25] J.Tauc, R.Grigorovici, A.Yancu; Phys.Stat.Sol., **15**, 627 **(1966)**.

[26] R.H.Bube; Electronic Properties of Crystalline Solids, Academic Oress, London, **(1974)**.